American Journal of Biological Anthropology

WILEY

AMERICAN JOURNAL OF BIOLOGICAL ANTHROPOLOGY
The Official Journal of the American Association of Biological Anthropologists

RESEARCH ARTICLE

Multisegment Model for Body Surface Area and Body Volume Estimation

Pavla A. Jarešová[1] | Martin Hora[1] | Michal Struška[1] | Tobias L. Kordsmeyer[2] | Julia Stern[3] | Lars Penke[2] | Vladimír Sládek[1]

[1]Department of Anthropology and Human Genetics, Charles University, Prague, Czech Republic | [2]Department of Psychology & Leibniz ScienceCampus Primate Cognition, University of Goettingen, Goettingen, Germany | [3]Department of Psychology, University of Bremen, Bremen, Germany

Correspondence: Vladimír Sládek (sladekv@yahoo.fr)

Received: 4 March 2025 | **Revised:** 12 February 2026 | **Accepted:** 13 April 2026

Keywords: 3D whole-body scans | anthropometry | body segments | geometric solids

ABSTRACT

Objectives: Body surface area (BSA) and body volume (BV) are crucial for understanding variations in body size and shape in humans. Direct measurement of BSA and BV is challenging due to the complex human body shape and variation in body proportion and composition among humans. To address these limitations, we developed a multisegment model for estimating BSA and BV.

Materials and Methods: The multisegment model of the human body divides the body into eight segments, each represented by geometric solids determined by linear dimensions. The trunk segment was represented as a circular base cylinder, an elliptical base cylinder, and a cuboid to determine the most accurate trunk representation. BSA and BV were computed by summing the surface areas and volumes of these geometric solids. The estimation error of our multisegment model and the previous models was tested using 60 3D whole-body scans of males.

Results: Models with circular and cuboidal trunk shapes provide more accurate BSA estimates compared to the elliptical trunk model, while the cuboidal trunk model was the most accurate for BV estimation. Our cuboidal trunk model showed a similar estimation error for BSA but reduced the error for BV estimates by at least 5 percentage points compared to previously published models.

Discussion: Our model stresses the importance of accurate representation of the trunk segment with three different representations. The estimate of BSA has better accuracy than the BV estimate. The model's overall accuracy highlights its potential for broader applications in anthropological and physiological research.

1 | Introduction

Body surface area (BSA) and body volume (BV) play important roles in understanding processes related to variation in body size and shape in past and present humans. Body surface area and body volume are scaling variables for physiological processes (Hosey-Cojocari et al. 2021; Peters and Glass 2010; Vauthey 2002) and are used in the medical field in the treatment of burn injuries (Moore et al. 2024; Retrouvey et al. 2018) and drug dosing (Crawford et al. 1950; Pinkel 1958); but see (Felici et al. 2002; Mathijssen et al. 2007; Pai 2012). However, body surface area and body volume are also used in evolutionary and ecological studies related to human variation, explaining aspects such as thermoregulation, human ecogeographic differences (Blackburn and Hawkins 2004; Hora et al. 2020; Ruff 1991; Wheeler 1992), or changes in body size and shape during human evolution (Collard and Cross 2017; Hora et al. 2022, 2020; Ruff 1993; Ruxton and Wilkinson 2011; Wheeler 1984).

Direct measurements of body surface area and body volume are not straightforward, given the complicated shape of the human body and the variation in body proportions and body composition. Techniques of direct measurement of body surface area, such as the coating method (Abernethy 1793), triangulation (Custor 1873; Fubini and Ronchi 1881), and planimetry (Roussy 1899) are labor-intensive (Brožek et al. 1987; Tikuisis et al. 2001) with questionable reproducibility (Brožek et al. 1987) as well as questionable ethics (e.g., skinning a cadaver, Sappey 1852). Direct measurements of body volume using, for example, the water displacement technique (Robertson 1757), also resulted in difficulties with accuracy (Brožek et al. 1987), and the underwater weighing method was impracticable in some cases (Siri 1961). Methods of direct measurement of body volume are generally not within the scope of the average clinical laboratory (Wakat et al. 1971). Moreover, further development of direct body surface area and body volume measurements using more sophisticated technical instruments, such as surface scanners (Dechenaud et al. 2021; Tikuisis et al. 2001) and photogrammetry (Pierson 1962), is limited due to their financial and time feasibility.

The main attempt to estimate body surface area and body volume so far was based on indirect techniques using regression equations. That is, the most frequent estimations of body surface area were based on regression equations using stature and body mass (Boyd 1935; DuBois and DuBois 1916; Gehan and George 1970; Haycock et al. 1978; Mosteller 1987; Yu et al. 2010). Body volume estimations were based on regression equations using stature, body mass, and body density (Sendroy and Cecchini 1959; Sendroy and Collison 1966; Wakat et al. 1971). Both stature and body mass are relatively easy to obtain from living humans, but body density is more complicated, given variation in body composition and individual fluctuation, and age-related changes between lean body mass and fat tissue (Krzywicki and Chinn 1967; Sendroy and Cecchini 1959; Sendroy and Collison 1966).

The regression equations for body surface area and body volume using stature and body mass were also applied to skeletal samples and fossil record (Churchill 2006; Collard and Cross 2017; Ruff 1993; Stibel 2023); however, in these, some of the limitations observed in living humans were even more accentuated and had a larger impact on the resulting accuracy. While stature can be estimated from bones with reasonable accuracy (percent prediction error $<2\%$), body mass can be affected by an error even larger than 20% (Ruff et al. 2012; Ruff and Wood 2023). Another factor influencing the accuracy of final body volume and surface area taken from the skeleton is preservation. Techniques with the highest accuracy, such as an anatomical reconstruction of stature (Maijanen 2009; Raxter et al. 2006) and bi-iliac breadth and stature for body mass estimation (Ruff and Wood 2023), are the most sensitive to the degree of preservation. Moreover, stature and body mass showed allometric variation among past populations due to differences in subsistence and ecological changes (Ruff and Wood 2023). Similarly, estimating body density from skeletal records is challenging, primarily due to the unknown variation in the proportion of lean body mass to fat among past populations.

For body surface area and body volume estimation, body proportionality is often discussed regarding thermoregulation and ecogeographic rules (Bogin et al. 2022; Churchill 2006; Geist 1990; Katzmarzyk and Leonard 1998; Ocobock 2024; Pomeroy et al. 2021; Ruff 1994). The effect of variation in body proportions on body surface area among human populations was partly solved using a geometric approach and a multisegment technique (Cross et al. 2008; Kasabova and Holliday 2015; Ruff 1991, 1993, 1994). The geometric approach for estimating body surface area was applied in Ruff's model using stature and bi-iliac breadth for computation (Ruff 1991, 1993, 1994). This model reflects variation in bi-iliac breadth and its effect on the body surface area to body volume ratio. In the multisegment technique, the body segments are represented by geometric solids that also reflect the variability in upper and lower limb proportions (Cross et al. 2008; Kasabova and Holliday 2015). Each geometric solid can be defined by its length and radii (Kasabova and Holliday 2015) or circumferences (Cross et al. 2008), which are measured either by standard somatometric techniques on living humans (Cross et al. 2008) or osteometric approaches from the skeletal record (Kasabova and Holliday 2015). Finally, body surface area and body volume are computed using the sum of surface areas and volumes of each segment (Kasabova and Holliday 2015).

The key limitation in the geometric approach and multisegment technique is the fact that it has been developed using values of body surface area and body volume derived from stature and body mass, rather than being directly measured on the body from which linear measurements were taken (Kasabova and Holliday 2015; Ruff 1991). Moreover, body volume was approximated by body mass, but the density of different tissues of the body was replaced by the mean body density taken from medical research (Kasabova and Holliday 2015). Finally, some multisegment models so far have not included certain segments, such as the foot, or did not study each body part as an individual segment (Kasabova and Holliday 2015).

The goal of our paper is to develop a multisegment model for the estimation of body surface area and body volume, testing its accuracy using 3D body scans. We divided the human body into eight individual segments represented by simple geometric solids, with the division of upper and lower limbs into separate parts, including the foot. We tested the approximation for trunk shape by three different geometric solids: a cylinder with a circular base, a cylinder with an elliptical base, and a cuboid. Body surface area and body volume were computed by summing selected geometric solids whose surface area and volume were calculated using linear dimensions obtained from surface scans of the human body. Computed body surface area and body volume were tested against the "true value" measured directly on the human body, taken from surface scans. Finally, we tested the agreement among previous techniques used for body surface area and body volume estimation (DuBois and DuBois 1916; Kasabova and Holliday 2015; Ruff 1991).

2 | Material and Methods

2.1 | Sample

Our sample, selected from Kordsmeyer and Penke (2019), consisted of young adult males ($n = 60$; mean age: 24.6 ± 3.2 years, mean stature: 180.1 ± 10.0 cm, mean body mass: 78.1 ± 14.4 kg).

The sample is further characterized in Table 1 (see also Kordsmeyer et al. 2018; Kordsmeyer and Penke 2019). Participants were mostly students from the University of Göttingen (Germany) of European origin. This study was approved by the Georg-Elias-Müller-Institute of Psychology's Ethics Committee (no. 111).

TABLE 1 | Sample description.

	Mean	SD	Minimum	Maximum
Age (years)	24.6	3.2	18.0	34.0
Stature (cm)	180.1	10.0	159.7	201.2
Body mass (kg)	78.1	14.4	52.7	109.8
BMI (kg/m^2)	24.0	3.8	17.1	35.9
Bi-iliac breadth (cm)	32.0	2.6	27.9	37.7
Lower limb length (cm)	79.4	5.4	67.9	92.0
Body surface area (m^2)	1.9	0.2	1.5	2.4
Body volume (dm^3)	78.8	14.3	52.4	111.3

Note: BMI denotes body mass index. Lower limb length is defined as the sum of thigh length (as defined in Table 4) and the distance of the *Tibiale externum* point from the ground.

2.2 | Multisegment Model

Our model for estimation of body surface area and body volume consists of three central segments (head, neck, and trunk) and five bilateral segments (upper arm, forearm, thigh, lower leg, and foot), and is visualized in Figure 1. Each body segment was represented by a geometric solid. The head segment was modeled as a sphere, and the neck segment as a cylinder. We modeled three variants of the trunk segment: (1) circular trunk as a cylinder with a base of a circle (model with circular trunk), (2) elliptical trunk as a cylinder with the base of an ellipse (model with elliptical trunk), and (3) cuboidal trunk as a cuboid (model with cuboidal trunk). The upper arm, thigh, and lower leg were modeled as a cylinder, the forearm as a conical frustum, and the foot segment as a half-cylinder. Equations for the estimation of segmental surface area and segmental volume are provided in Table 2. Surface areas of segments modeled as a cylinder, cuboid, and conical frustum (neck, trunk, upper arm, forearm, thigh, and lower leg) excluded the bases. In head surface area, we subtracted the base of the neck segment to account for the articulation of the head and neck. In foot surface area, we subtracted the distal base of the lower leg segment to account for the articulation of the lower leg and foot (Table 2). We excluded the hand as an individual segment from our model due to the impossibility of measuring its surface area and volume on our body scans, resulting in the omission of approximately 5% of the total body surface area (Hsu and Yu 2010; Lee et al. 2007; Yu et al. 2008; refer to Table 3 for relative hand surface area values from literature) and 1.3% of the body volume (Kasabova

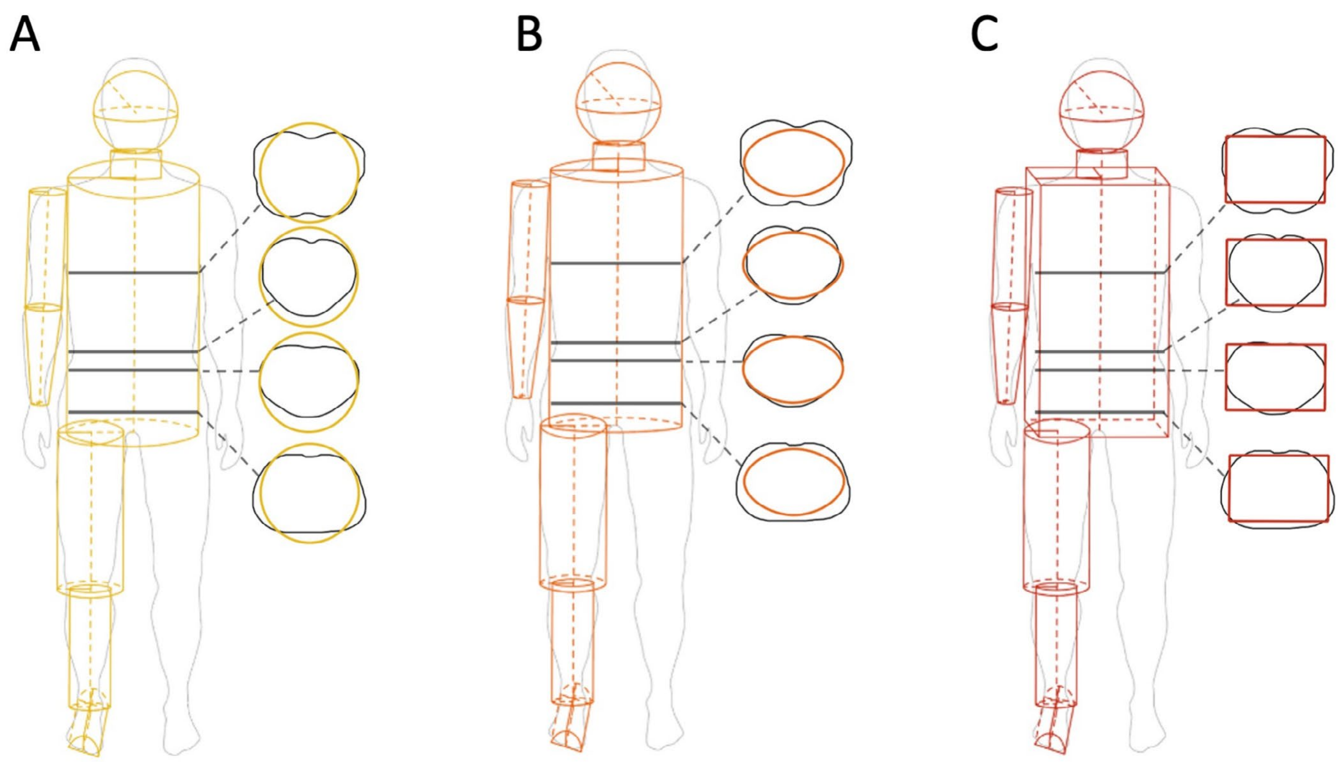

FIGURE 1 | Multisegment model with trunk variants. Presented model variants with trunk segment cross-sections of one representative individual at level of the chest circumference in the normal position (M 61) (first row), waist level (M 62) (second row), level of the point iliocristale (third row), and level of hip circumference (M 64(1)) (fourth row) interleaved on the outline of the circular model (A), elliptical model (B), and cuboidal model (C).

TABLE 2 | Equations for calculation of the surface area and volume of segments.

Segment	Surface area	Volume
Head	$S_{head} = 4\pi {r_{head}}^2 - \pi {r_{neck}}^2$	$V_{head} = \frac{4}{3}\pi {r_{head}}^3$
Neck	$S_{neck} = 2\pi r_{neck} h_{neck}$	$V_{neck} = \pi {r_{neck}}^2 h_{neck}$
Circular trunk	$S_{circulartrunk} = 2\pi r_{ml} h_{trunk}$	$V_{circulartrunk} = \pi {r_{ml}}^2 h_{trunk}$
Elliptical trunk	$S_{ellipticaltrunk} = \pi \frac{3}{2}\left(r_{ml} + r_{ap}\right) - \sqrt{r_{ml} r_{ap}} h_{trunk}$	$V_{ellipticaltrunk} = \pi r_{ml} r_{ap} h_{trunk}$
Cuboidal trunk	$S_{cuboidaltrunk} = 2\left(2 r_{ml} h_{trunk} + 2 r_{ap} h_{trunk}\right)$	$V_{cuboidaltrunk} = 2 r_{ml} 2 r_{ap} h_{trunk}$
Upper arm	$S_{upperarm} = 2\pi r_{upperarm} l_{upperarm}$	$V_{upperarm} = \pi {r_{upperarm}}^2 l_{upperarm}$
Forearm	$S_{forearm} = \pi\left(r_{upperarm} + r_{forearm}\right)\sqrt{{l_{forearm}}^2 + \left(r_{upperarm} - r_{forearm}\right)^2}$	$V_{forearm} = \frac{\pi l_{forearm}}{3}\left({r_{upperarm}}^2 + r_{upperarm} r_{forearm} + {r_{forearm}}^2\right)$
Thigh	$S_{thigh} = \pi r_{thigh} l_{thigh}$	$V_{thigh} = \pi\left(\frac{r_{thigh}}{2}\right)^2 l_{thigh}$
Lower leg	$S_{lowerleg} = 2\pi r_{lowerleg} l_{lowerleg}$	$V_{lowerleg} = \pi {r_{lowerleg}}^2 l_{lowerleg}$
Foot	$S_{foot} = \pi r_{foot}\left(r_{foot} + l_{foot}\right) + 2 r_{foot} v_{foot} - \pi {r_{ankle}}^2$	$V_{foot} = \frac{\pi {r_{foot}}^2 l_{foot}}{2}$

Note: For the definition of abbreviations, see Table 4.

TABLE 3 | Relative hand surface area from literature.

Study	Sample size	Hand surface area (%BSA)	SD	Studied sample
Tikuisis et al. (2001)	12	2.48	0.46	Italy, Netherlands, USA
Yu et al. (2008)	135	2.39	0.23	Taiwan
Lee et al. (2007)	34	2.46	0.19	South Korea

Note: All referenced samples are males.

and Holliday 2015). To incorporate each hand segment into the whole-body surface area and volume estimate, we calculated hand surface area and volume so that they accounted for 2.5% of the body surface and 0.65% of the body volume. Estimated body surface area and estimated body volume were obtained by summing the calculated surface areas and volumes of individual segments, respectively.

2.3 | Imaging

The true values for body surface area and body volume were obtained from surface scanning images. Each participant was scanned using a Vitus^{smart}XXL scanner (Human Solutions GmbH, Kaiserslautern, Germany) with a cubic scanning volume according to the DIN EN ISO 20685 with a data density of 27 points/cm^2 (Bretschneider et al. 2009; Kordsmeyer et al. 2019). Each participant wore tight underwear (Kordsmeyer et al. 2019). During a 10-s scan, participants were instructed to breathe normally. Each participant was standing straight with legs hip-width apart, upper limbs stretched out and held slightly away from the body, making fists with the thumbs pointing forward, and head in line with the Frankfort horizontal (for a detailed description of the scanning protocol, see Kordsmeyer et al. 2019).

2.4 | Measurements

Surface, volume, and individual measurements were taken from surface scans using the 3D Measure Up V software (ver. 2.2, ProtoTech Solutions, Pune, Maharashtra, India). All measurements were taken by a single observer; therefore, interobserver error does not affect the presented results. The coefficient of variation of all measurements was below 3%, indicating a suitable level of accuracy for practical application. True values for surface area and volume were taken either from the whole body or from each segment defined in Figure 1. Surface and volume for segments were taken between measured planes placed at the boundary between two segments. Finally, estimated surface areas and volumes were computed from equations representing geometric properties of each segment (Table 4) using 17 anthropometric measurements, following the technique described by Knussmann (1988).

2.5 | Analyses

We tested the accuracy of our estimates of segmental surface areas, segmental volumes, body surface area, and body volume relative to scanned values using Pearson's correlation coefficient, reduced major axis regression in linear and logarithmic space, mean percentage difference, mean percentage absolute difference, and standard error of the estimate. The reduced major axis (RMA) regression analysis was chosen here over the ordinary least squares regression or major axis regression, as it is preferable when the variables on both axes are subject to error (Aiello 1992; Sokal and Rohlf 1995). To determine if the ratio between estimated and scanned values is isometric, we assessed whether the slope given by the RMA regression equation

TABLE 4 | Body dimensions.

Dimension	Abbreviation	Description
Head radius	r_{head}	Half of the distance between *glabella* and *opisthocranion* points (M 1)
Neck radius	r_{neck}	Calculated from the measured neck circumference (M 63) using the formula: $r_{neck} = \frac{C_{neck}}{2\pi}$, where C_{neck} is the circumference of the neck
Trunk mediolateral radius	r_{ml}	Half of the bi-iliac breadth (M 40)
Trunk anteroposterior radius	r_{ap}	Half of the distance between *iliospinale anterius* and *iliospinale posterius* points [M 43(1)]
Upper arm radius	r_{UA}	Half of the biepicondylar width of the humerus [M 52(3)]
Forearm distal radius	$r_{forearm}$	Half of the distal diameter of the forearm [M 52(4)]
Thigh radius	r_{thigh}	Quarter of the bi-iliac breadth (M 40)
Lower leg radius	$r_{lower\ leg}$	Half of the distance between *merion laterale* and *merion mediale* points (M 59d)
Foot half-cylinder radius	r_{foot}	Half of the distance of the *supratarsale tibiale* point from the ground
Radius of subtracted circle	r_{ankle}	Half of the distance between *supratarsale tibiale* and *supratarsale fibulare* points (M 59e) which is the radius of the circle whose contents have been deducted due to the segment's connection to the lower leg segment
Neck height	h_{neck}	Determined by subtracting the distances of the *gnathion* point from the ground [M 3(1)] and of the *cervicale* point from the ground (M 19)
Trunk height	h_{trunk}	Determined by subtracting the distance of the *cervicale* point from the ground (M 19) and the sum of the thigh segment length (l_{thigh}) and the distances of the *tibiale externum* point from the ground
Upper arm length	l_{UA}	Upper arm length (M 47)
Forearm length	$l_{forearm}$	Forearm length
Thigh length	l_{thigh}	Determined by subtracting the distances of the *iliospinale anterius* point from the ground (M 13) and of the *tibiale externum* point from the ground which determined the value from which we subtracted 7% to obtain the length of the femur (Fetter et al. 1967), from which we subtracted 27% of the length to obtain the final length of the thigh segment, as roughly this portion of the femur occurs above the crotch area and is therefore assigned to the trunk segment (Collard and Cross 2017; Cross et al. 2008)
Lower leg length	$l_{lower\ leg}$	Determined by subtracting the distances of the *tibiale externum* point from the ground and of the *supratarsale tibiale* point from the ground
Foot length	l_{foot}	Foot length (M 58)

Note: Labels in parentheses correspond to the numbering system used in Knussmann (1988).

in logarithmic space differs from 1.0 based on the confidence interval and p value. We also calculated the surface area and volume of individual segments relative to the whole body. We calculated the mean percentage difference (MD%) to assess overestimation and underestimation, and the mean percentage absolute difference (MAD%) to assess the accuracy following Sládek et al. (2010) as follows:

$$\mathrm{MD}\% = \frac{\sum_{i=1}^{n}\left[\left(EV_{\mathrm{i}} - SV_{\mathrm{i}}\right)/SV_{\mathrm{i}}\right]\cdot 100}{n}, \quad (1)$$

$$\mathrm{MAD}\% = \frac{\sum_{i=1}^{n}\left[EV_{\mathrm{i}} - SV_{\mathrm{i}}\right|/SV_{\mathrm{i}}]\cdot 100}{n}, \quad (2)$$

where EV is the estimated value, SV is the scanned value, and n is the number of participants. The MD% corresponds to the bias parameter in the Bland–Altman analysis when the differences between methods are expressed as percentages of the true value. Additional Bland–Altman parameters are presented in Figure S1. To assess the biological importance of MAD%, we compared the absolute units given by MAD% with the standard deviation of BSA and BV, respectively. We calculated the standard error of estimate (%SEE) in order to be able to compare this value given by previous models on our dataset with that previously published, following Pineau and Ramirez Rozzi (2022), as follows:

$$\%\mathrm{SEE} = \left(\frac{\sqrt{\frac{1}{n}\sum_{i=1}^{n}\left(SV_{\mathrm{i}} - EV_{\mathrm{i}}\right)^{2}}}{SV_{\mathrm{i}}}\right)\cdot 100 \quad (3)$$

All statistical analyses were done in Microsoft Excel and Past 4.01.

3 | Results

Segmental surface area estimation statistics are given in Table 5. Plots of the estimated segmental surface area against scanned segmental surface area in logarithmic space are shown in Figure 2. Segmental surface area estimates were significantly correlated with the scanned segmental surface area (Pearson's r: 0.652–0.903; $p < 0.001$), with the lowest correlation coefficients being in the head ($r = 0.715$) and upper arm ($r = 0.652$). The estimated segmental surface areas of the head, trunk, forearm, thigh, lower leg, and foot were isometric to the scanned segmental surface area. The estimated surface area of the upper arm segment showed negative allometry, and the estimated neck segmental surface area showed positive allometry. Segmental surface area was overestimated in the circular trunk, cuboidal trunk, and thigh as indicated by positive MD% ($p < 0.001$) and underestimated in all other segments as indicated by negative MD% ($p < 0.001$). All segments had MAD% significantly different from zero ($p < 0.001$). The MAD% between the estimated and scanned segmental surface area was 6%–10% for most of the segments except for the elliptical trunk (13%), head (15%), and neck (33%).

Segmental volume estimation statistics are given in Table 6. Plots of the estimated segmental volume against scanned segmental volume in logarithmic space are shown in Figure 3. Segmental volume estimates were correlated with the scanned segmental volume (Pearson's $r > 0.621$; $p < 0.001$), especially for the trunk and neck segments (Pearson's $r = 0.898$–0.914; $p < 0.001$). The estimated segmental volumes of the head, neck, trunk, forearm, thigh, lower leg, and foot were isometric to the scanned segmental surface area. The estimated volume of the upper

TABLE 5 | Statistics for estimation of the surface area of segments of our model.

Model	Pearson's r	RMA regression	Log slope (CI)	MD% (SD)	MAD% (SD)	%SEE
Head	0.715***	$y = 0.7002x + 214.040$	0.844 (0.633; 1.017)	−14.90 (7.01)***	14.93 (6.94)***	17.27
Neck	0.807***	$y = 0.7792x - 24.339$	1.235 (1.026; 1.410)*	−32.57 (12.31)***	32.57 (12.31)***	36.80
Circular trunk	0.898***	$y = 1.0263x + 86.702$	0.988 (0.852; 1.085)	4.01 (5.46)***	5.69 (3.68)***	6.75
Elliptical trunk	0.892***	$y = 0.8719x - 35.281$	1.008 (0.873; 1.110)	−13.19 (4.75)***	13.19 (4.75)***	14.40
Cuboidal trunk	0.889***	$y = 1.1030x - 83.874$	1.014 (0.871; 1.119)	9.26 (6.08)***	9.52 (5.68)***	10.99
Upper arm	0.652***	$y = 0.5421x + 322.670$	0.642 (0.431; 0.778)*	−5.11 (11.23)***	8.79 (8.66)***	16.63
Forearm	0.903***	$y = 0.9816x - 39.661$	1.074 (0.940; 1.199)	−8.60 (4.79)***	8.67 (4.65)***	10.01
Thigh	0.769***	$y = 1.1282x - 118.700$	1.044 (0.855; 1.198)	5.86 (8.64)***	8.12 (6.56)***	10.34
Lower leg	0.873***	$y = 1.0179x - 60.088$	1.058 (0.896; 1.180)	−3.28 (6.46)***	6.16 (3.82)***	7.38
Foot	0.826***	$y = 1.1757x - 124.740$	1.249 (0.993; 1.456)	−3.94 (6.86)***	6.09 (5.05)***	7.83

Note: Pearson's r is the result of correlation between estimated surface area and scanned surface area; Equation of reduced major axis regression; Log slope (CI), slope of reduced major axis regression equation in logarithmic space with confidence interval of the slope; MD%, mean percentage difference; MAD%, mean percentage absolute difference; %SEE, standard error of estimate; For Pearson's r, MD%, and MAD% the asterisks denote significant difference from zero; For Log slope the asterisk denotes significant difference from 1. Levels of significance are labeled as follows: *$p < 0.05$, **$p < 0.01$, ***$p < 0.001$.

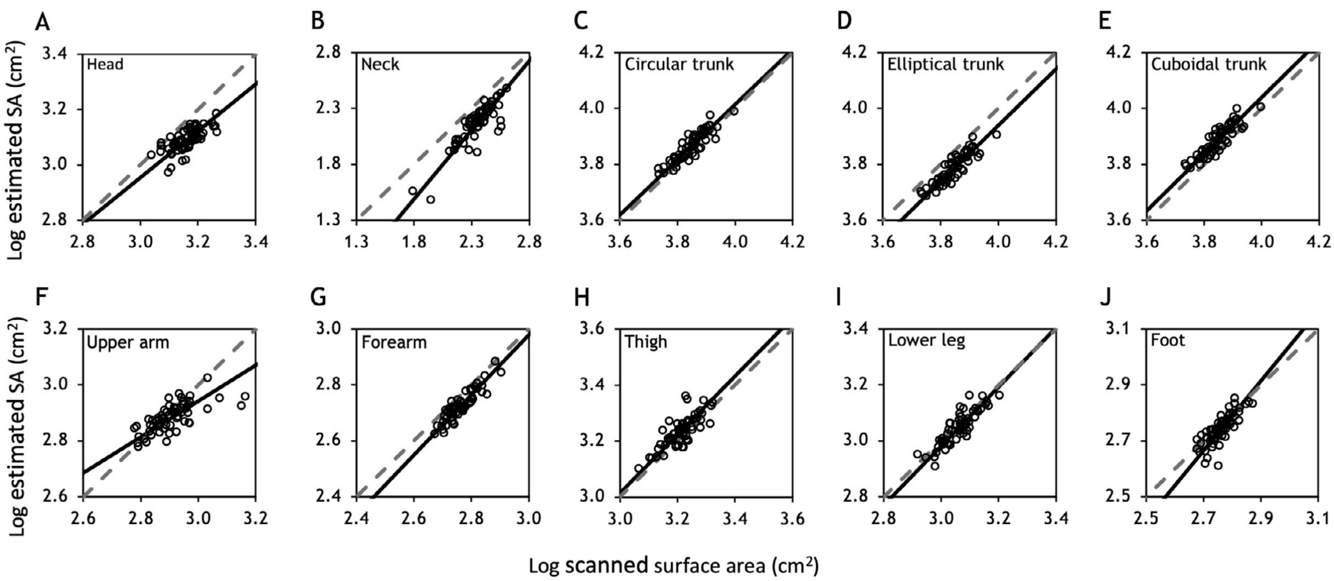

FIGURE 2 | RMA regression plot of estimated surface area (SA) against scanned SA in logarithmic space for individual segments. The dashed line represents a hypothetical isometric model.

arm segment showed negative allometry. Our models overestimated the volume of the circular trunk, cuboidal trunk, and thigh, as indicated by positive MD% ($p<0.001$), and underestimated all other segments, as indicated by negative MD% values ($p<0.01$). All segments had MAD% significantly different from 0 ($p<0.001$). The MAD% between the scanned and estimated segment volume was below 10% for the head and cuboidal trunk, 10%–20% for most of the segments, and > 20% for circular trunk, upper arm, and foot.

Relative surface area and volume of scanned segments are given in Table 7. The trunk segment had the highest impact on both body surface area and body volume, accounting for 37% and 59%, respectively. The thigh segment had the second highest contribution, followed by the lower leg and upper arm segments. Among all segments, the neck contributed the least, representing roughly 1% of both body surface area and body volume.

Body surface area (BSA) estimation statistics are given in Table 8. Plot of the estimated BSA against scanned BSA in logarithmic space is shown in Figure 4. The results of the Bland–Altman analysis are presented in Figure S1. The estimated BSA of each tested model was highly correlated with the scanned BSA (Pearson's $r=0.928$–0.970; $p<0.001$). The estimated BSA of all models was isometric to the scanned BSA except the Ruff model (1991), which showed positive allometry. Our model with a circular trunk overestimated BSA by 1%, and the model with a cuboidal trunk by 3%, as indicated by positive MD% values, whereas the model with an elliptical trunk underestimated BSA by 6%. All previously published models had positive MD% and thus overestimated the BSA by 4%–6% ($p<0.001$). All models had MAD% significantly different from 0 ($p<0.001$). Estimates of BSA from our circular-trunk model had the lowest MAD%, followed by those from our cuboidal-trunk model and the previously published models. Our model with an elliptical trunk had the highest MAD% of all models.

TABLE 6 | Statistics for the estimation of the volume of segments of our model.

Model	Pearson's *r*	RMA regression	Log slope (CI)	MD% (SD)	MAD% (SD)	%SEE
Head	0.692***	$y=0.8606x+486.960$	0.908 (0.728, 1.059)	−3.51 (9.76)**	7.83 (6.80)***	11.39
Neck	0.910***	$y=0.9144x-20.177$	1.077 (0.892, 1.209)	−11.72 (12.07)***	12.91 (10.79)***	17.64
Circular trunk	0.914***	$y=1.2049x+2959.600$	0.927 (0.794, 1.033)	27.60 (10.97)***	27.60 (10.97)***	28.73
Elliptical trunk	0.898***	$y=0.8206x+198.210$	0.974 (0.833, 1.107)	−17.07 (8.20)***	17.61 (6.96)***	19.80
Cuboidal trunk	0.898***	$y=1.0448x+252.370$	0.974 (0.828, 1.098)	5.59 (10.44)***	9.08 (7.61)***	10.82
Upper arm	0.760***	$y=0.6486x+222.180$	0.869 (0.745, 0.990)*	−22.59 (10.30)***	22.64 (10.20)***	27.48
Forearm	0.802***	$y=0.8411x+69.544$	0.927 (0.774, 1.060)	−7.86 (11.16)***	11.26 (7.71)***	14.85
Thigh	0.768***	$y=1.1892x-228.870$	0.994 (0.821, 1.325)	16.08 (15.18)***	17.96 (12.90)***	21.17
Lower leg	0.799***	$y=0.9824x-116.190$	1.077 (0.899, 1.207)	−5.29 (12.13)**	11.19 (7.05)***	13.86
Foot	0.621***	$y=0.8776x-74.510$	1.189 (0.879, 1.446)	−20.39 (10.90)***	20.49 (10.69)***	25.28

Note: For description of symbols and variables see Table 5.

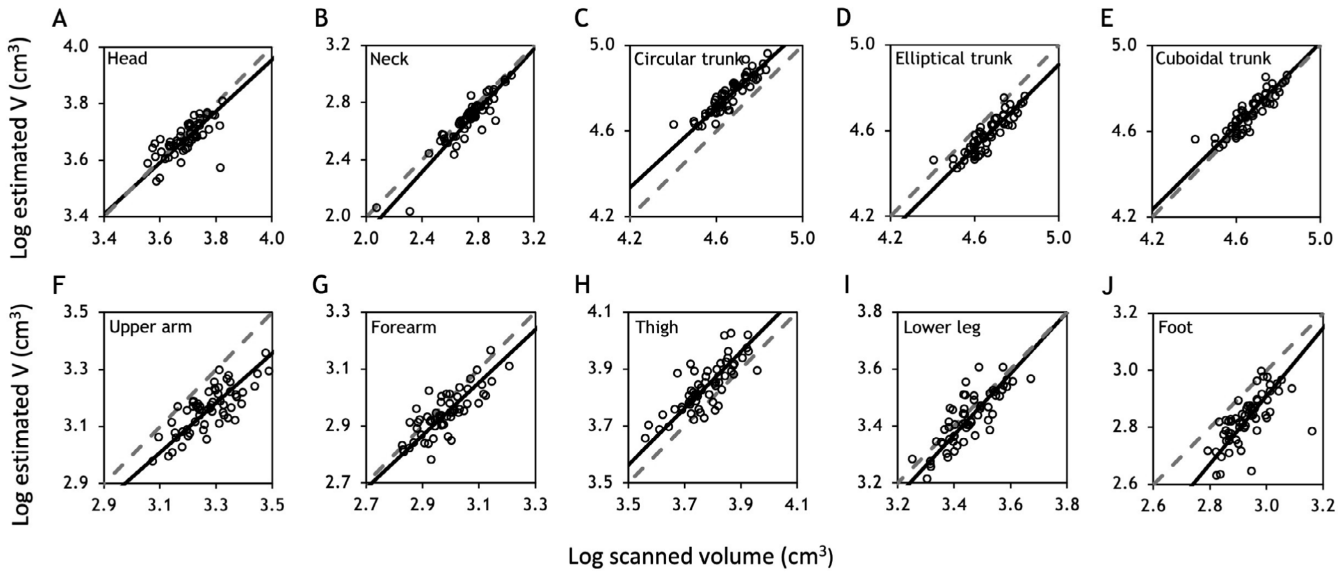

FIGURE 3 | RMA regression plot of estimated volume (V) against scanned V in logarithmic space for individual segments. The dashed line represents a hypothetical isometric model.

Body volume (BV) estimation statistics are provided in Table 9. The plot of the estimated BV against scanned BV in logarithmic space is shown in Figure 5. The results of the Bland–Altman analysis are presented in Figure S1. The estimated BV of each tested model was highly correlated with the scanned BV (Pearson's $r = 0.915$–0.939; $p < 0.001$). The estimated BV of all models was isometric to the scanned BV. The model with a cuboidal trunk had the MD% closest to 0%. The model with an elliptical trunk and the Kasabova and Holliday model (Kasabova and Holliday 2015) underestimated BV, and the model with a circular trunk and the Ruff model (Ruff 1991) overestimated the BV. The MAD% of our model with a cuboidal trunk (6%) was lower than in our other models (10%–16%) and in previously published models by Kasabova and Holliday (2015; 11%), and Ruff (1991; 86%). Comparison of MAD% with the standard deviation of scanned volume showed that the MAD% of the model with an elliptical and cuboidal trunk is smaller than the standard deviation. The model with a circular trunk had MAD% larger than the standard deviation.

4 | Discussion

We have presented a new technique for estimating body surface area and body volume and tested it using 3D whole-body scans using a multisegment model with circular, elliptical, and cuboidal geometric approximations for the trunk. Body surface area was overestimated by the circular-trunk model by 1% and by the cuboidal-trunk model by 3%, respectively, and it was underestimated by the elliptical-trunk model by 6%. For body volume, the model with a cuboidal trunk overestimates BV by 3%, and the model with an elliptical trunk by 10%. The model with a circular trunk overestimates BV by 17% and therefore does not seem suitable for BV estimation. Individual body segments differ in their contribution to BSA and BV, with the trunk segment having the most important impact, making a crucially accurate estimation of trunk segmental surface area and segmental volume.

Previous studies used a cylinder with a circular base for modeling the trunk segment in BSA and BV estimations (Cross et al. 2008; Kasabova and Holliday 2015; Ruff 1991, 1993, 1994). However, Kasabova and Holliday (2015) proposed that an elliptical trunk base would provide a more accurate estimate of BSA and BV, due to the anteroposteriorly flattened chest. Our results suggest that a trunk with a circular shape provides a more accurate estimation of BSA, but a less accurate estimation of BV, compared to a trunk with an elliptical shape. The anteroposteriorly flattened thorax is also reflected

TABLE 7 | Relative surface area and volume of body segments.

	Relative surface area (% of BSA)	Relative volume (% of BV)
Head	7.60	6.50
Neck	1.22	0.76
Trunk	36.61	59.04
Upper arm	4.27	2.46
Forearm	3.02	1.24
Thigh	8.51	7.72
Lower leg	5.98	3.66
Foot	3.01	1.12

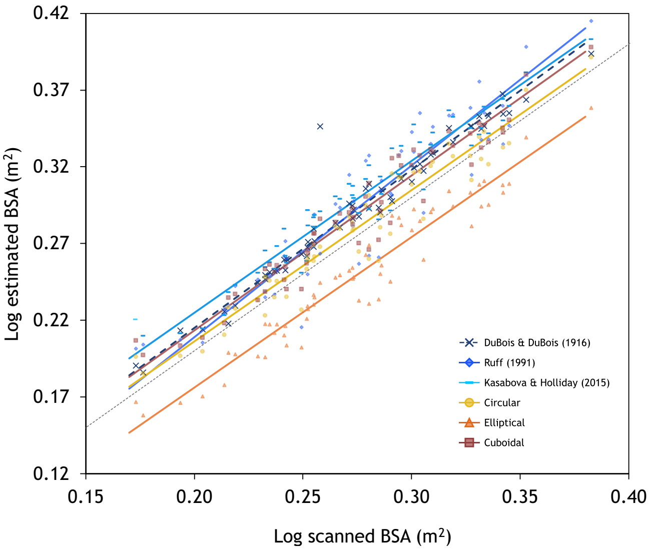

FIGURE 4 | RMA regression plot of estimated body surface area (BSA) against scanned BSA for present and previous models in logarithmic space. The black dashed line represents a hypothetical isometric model.

TABLE 8 | Statistics for estimation of the body surface area by present and previous models.

Model	Pearson's r	RMA regression	Log slope (CI)	MD% (SD)[a]	MAD% (SD)	%SEE
Circular	0.964***	$y = 1.0227x - 0.0259$	0.985 (0.915, 1.050)	1.00 (2.74)**	2.53 (1.45)***	2.95
Elliptical	0.965***	$y = 0.9462x - 0.0081$	0.980 (0.910, 1.043)	−5.75 (2.48)***	5.75 (2.48)***	6.36
Cuboidal	0.963***	$y = 1.0502x - 0.0388$	1.009 (0.937, 1.073)	3.06 (2.79)***	3.56 (2.12)***	4.15
DuBois and DuBois (1916)	0.970***	$y = 1.0707x - 0.0595$	1.030 (0.971, 1.073)	3.96 (2.74)***	3.96 (2.74)***	4.79
Ruff (1991)	0.928***	$y = 1.1942x - 0.2885$	1.119 (1.015, 1.211) *	4.18 (4.44)***	5.18 (3.22)***	6.30
Kasabova and Holliday (2015)	0.963***	$y = 1.0467x + 0.0175$	0.989 (0.914, 1.055)	5.67 (2.89)***	5.67 (2.89)***	6.30

Note: For description of symbols and variables see Table 5.
[a]MD% values correspond to the bias parameter from the Bland–Altman analysis, as presented in Figure S1.

TABLE 9 | Statistics for estimation of the body volume by present and previous models.

Model	Pearson's *r*	RMA regression	Log slope (CI)	MD% (SD)[a]	MAD% (SD)	%SEE
Circular	0.935***	$y = 1.1509x + 0.8392$	0.970 (0.871, 1.050)	16.45 (7.27)***	16.49 (7.18)***	17.80
Elliptical	0.937***	$y = 0.8766x + 1.4091$	0.968 (0.870, 1.048)	−10.30 (5.63)***	10.42 (5.40)***	12.33
Cuboidal	0.933***	$y = 1.0292x + 0.0851$	0.983 (0.880, 1.063)	3.28 (6.75)***	6.11 (4.35)***	7.36
Ruff (1991)	0.915***	$y = 1.9837x - 9.7968$	1.038 (0.916, 1.134)	86.12 (13.76)***	86.12 (13.76)***	88.35
Kasabova and Holliday (2015)	0.939***	$y = 0.8342x + 3.9503$	0.940 (0.845, 1.022)	−11.24 (5.40)***	11.26 (5.36)***	13.26

Note: For description of symbols and variables see Table 5.
[a]MD% values correspond to the bias parameter from the Bland–Altman analysis, as presented in Figure S1.

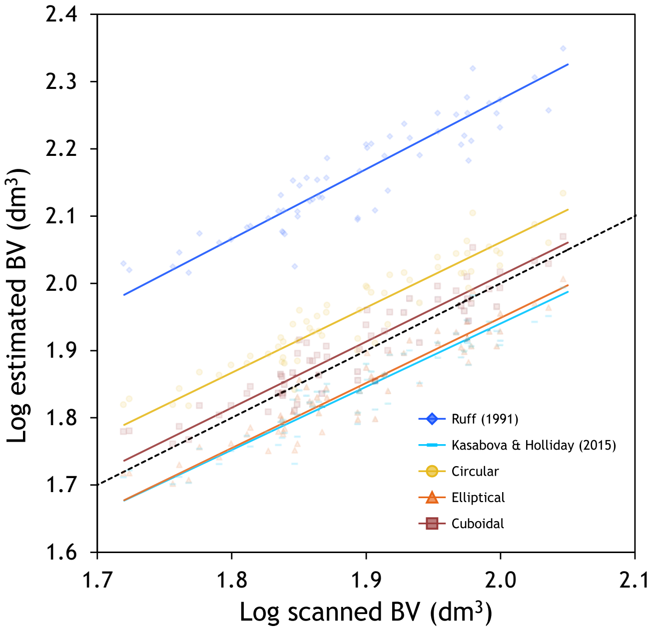

FIGURE 5 | RMA regression plot of estimated body volume (BV) against scanned BV for present and previous models in logarithmic space. The black dashed line represents a hypothetical isometric model.

by the representation by cuboidal shape. Surprisingly, the cuboidal shape is the most accurate for estimating BV, although the circular shape is still the best option for estimating BSA. Overall, the models with circular and cuboidal trunks are comparable when estimating BSA, and for BV, the model with a cuboidal trunk surpasses the others. The elliptical shape did not improve the accuracy of BSA and BV estimates and was the least accurate in our results. While accuracy is influenced by the measurements used in the model, the elliptical shape might perform differently if other dimensions were used instead of bi-iliac breadth and the distance between the anterior and the posterior superior iliac spines. We chose these dimensions for their reliable measurability in both living individuals and skeletal material, which would be challenging with other dimensions.

Estimates of trunk segmental surface area and volume are crucial for calculating BSA and BV, as the trunk accounts for 37% of BSA and 59% of BV. This substantial contribution results in similar trends in accuracy, underestimation, and overestimation between trunk surface area and volume estimations and overall BSA and BV estimations. This also implies that further improvement in BSA and BV estimations depends on improving the representation of the trunk segment, which could significantly enhance overall accuracy. The trunk segmental surface area is the most accurately estimated by the model with circular trunk shape (overestimates by 4%), followed by cuboidal trunk shape (overestimates by 9%). Regarding trunk segmental volume, the cuboidal trunk proves to be the most accurate (overestimates by 6%), while the circular trunk shape exhibits lower accuracy (overestimates by 28%). The overestimation observed in the circular and cuboidal trunk segmental surface area and volume is also reflected in the model's overestimation of BSA and BV, although the overestimation in whole-body estimates is less pronounced.

The segments other than the trunk exhibit varying levels of accuracy in surface area and volume estimation, with mean absolute percentage differences ranging from 6% to 15% for surface area and from 8% to 23% for volume. The thigh segment, along with the circular and cuboidal trunk segments, overestimates both surface area and volume. In contrast, the remaining segments generally underestimate their surface area and volume. The underestimation observed in these segments offsets the overestimation in the circular trunk, cuboidal trunk, and thigh segmental surface area and volume estimates. This balancing effect helps compensate for the pronounced overestimation in the trunk segment, resulting in a more accurate overall estimate of BSA and BV. However, issues arise when focusing on the surface area and volume of individual segments. While underestimation and overestimation counterbalance each other in BSA and BV estimates, this offset does not occur in segmental estimates. As a result, the use of segmental surface area and volume estimates may be inappropriate in certain instances, such as when assessing the effect of limb surface area-to-volume ratio in thermoregulatory studies. Nonetheless, the surface area estimates of limb segments tend to have less pronounced underestimation and overestimation compared to volume estimates, making the use of segmental surface area in heat loss calculations potentially feasible; but note that the upper arm showed a weaker estimated–scanned surface area correlation, likely reflecting soft-tissue variability (e.g., muscle and adipose tissue) that is not fully captured by the skeletal predictors.

A potential next step in the analysis of multisegmental models would be to evaluate how segment subdivision impacts the accuracy of body surface area and volume estimations. This could aim to determine the optimal number of segments required to maximize accuracy. Previous research has shown that body surface area and volume can be approximated using a simplified model that represents the body as a single cylindrical segment. However, our findings reveal that while this cylindrical model is well-suited to compute body surface area, it provides low accuracy for body volume. Furthermore, our results suggest that the accuracy of both body surface area and volume estimates could potentially be enhanced by separating the thoracic/abdominal region from the pelvic area and applying distinct geometric representations to each segment. This refined method not only addresses the limitations of the single-segment model but also raises questions about the impact of further body segmentation on estimation accuracy. Future research could explore the relationship between model complexity and accuracy, potentially revealing an optimal balance between segmentation detail and computational efficiency.

The main contribution of our analysis, however, is its testing against true values obtained from scanned surface area and volume values, rather than the estimated values used in Ruff (1991) and Kasabova and Holliday (2015), who relied on independently estimated body surface area and mass. A comparison of our model estimates with previous models' estimates of BSA shows that previous and our models have good accuracy, with MAD% between 2% and 6%. Our model's BV estimates, as well as the ones from Kasabova and Holliday (2015), have a comparable MAD% range of 6%–16%, whereas Ruff (1991) overestimates BV (MAD% = 86%). The large overestimation in Ruff's model, which visualizes the whole body as a single cylinder with a circular base, could be due to less matter around the head and lower limbs compared to the trunk, which influences the width of the cylinder used to model the whole body. Despite comparable accuracy among models, our circular-trunk and cuboidal-trunk models generally yield better BSA and BV estimates, respectively, across most test results.

Although our model has been tested only in living humans, most of the required anthropometric dimensions have a skeletal counterpart. Our model should therefore be applicable to skeletal material after soft-tissue adjustment or after testing its accuracy using whole-body CT scans. Additionally, a larger number of dimensions required by our model places a relatively high demand on the degree of preservation, or necessitates the use of equations to calculate missing dimensions. Thus, in terms of the number of dimensions required, it might be desirable to use the DuBois and DuBois equation using body height and body mass (DuBois and DuBois 1916), the Ruff model using body height and pelvic bi-iliac breadth (Ruff 1991), or Kasabova and Holliday (2015) model requiring body height and eight other dimensions measured (Kasabova and Holliday 2015). The applicability of the new model to skeletal material is also limited by the lack of an osteometric representation of the neck diameter. Since the neck segment accounts for less than 1% of the BSA and BV, we do not consider this problematic.

Our model was tested only on adult male bodies and may not be generalizable to female and non-adult bodies that deviate in size and proportions from our sample. Although our sample had a higher mean body mass (78 kg) and stature (180 cm) than any of the 31 male samples from diverse ecogeographic regions compiled by Ruff (1994; 43–76 kg, 145–175 cm) (Figure S2), individual variation in our sample overlaps with averages from 84% of these populations (excluding the five populations with the lowest body mass) and should be thus broadly representative of human male variation in overall body shape. More importantly, the accuracy of our models does not appear to be systematically influenced by body size or body proportions, as indicated by the absence of significant correlations between MD% and body mass, lower limb length/stature, trunk height/stature, or bi-iliac breadth/stature (Figures S3 and S4). These results indicate that our models are applicable to men from other populations with diverse body sizes and proportions and are thus useful for studying ecogeographical variation in BSA and BV. The robustness of our models to variation in body size and proportions also suggests that the balancing between overestimated and underestimated segments holds across this variation.

5 | Conclusions

This study presented a new model for estimating BSA and BV, comprising three variants that differ in the representation of trunk segments. The model variants were tested using 3D whole-body scans of living participants. Presented model variants allow for BSA and BV estimations as well as segmental surface area and volume estimations with varying accuracy. While the circular and cuboidal trunk and thigh segments tended to overestimate surface area and volume, other segments generally underestimated these metrics, resulting in higher accuracy of the presented model for whole-body estimation than for segmental estimations. This underscores challenges in applying segmental estimates, particularly in studies involving limb surface area to volume ratio in thermoregulation.

In conclusion, we recommend using models with circular and cuboidal trunks for BSA estimates, while the model with a cuboidal trunk is recommended for BV estimates. However, if BSA and BV need to be estimated together (e.g., in the case of computing the BSA-to-BV ratio), we recommend using the estimate based on the cuboidal-trunk model.

Author Contributions

Pavla A. Jarešová: conceptualization (lead), data curation (supporting), formal analysis (lead), methodology (equal), project administration (lead), visualization (equal), writing – original draft (lead), writing – review and editing (equal). **Martin Hora:** conceptualization (supporting), formal analysis (supporting), funding acquisition (equal), methodology (supporting), project administration (supporting), supervision (supporting), visualization (supporting), writing – original draft (supporting), writing – review and editing (equal). **Michal Struška:** formal analysis (supporting), visualization (supporting), writing – original draft (supporting), writing – review and editing (equal). **Tobias L. Kordsmeyer:** data curation (equal), methodology (equal), writing – review and editing (supporting). **Julia Stern:** data curation (equal), methodology (equal), writing – review and editing (supporting). **Lars Penke:** data curation (equal), methodology (equal), writing – review and editing (supporting). **Vladimír Sládek:** funding acquisition (equal), project administration (supporting), resources (equal), supervision (equal), visualization (supporting), writing – original draft (supporting), writing – review and editing (equal).

Acknowledgments

We would like to thank Erik Mitro for his help with statistical analysis. The project was supported by the Grant Agency of Czech Republic (EXPRO: 21-17092X: The Formation of Multi-ethnic Complex Societies in Early Medieval Moravia. Collective Action Theory and Interdisciplinary Approach). Martin Hora has been supported by the Charles University Research Centre program No. 204069.

Funding

This work was supported by the Charles University Research Centre (204069) and Grantová agentura České republiky (EXPRO: 21-17092X).

Conflicts of Interest

The authors declare no conflicts of interest.

Data Availability Statement

The data that support the findings of this study are available from the corresponding author upon request.

References

Abernethy, J. 1793. "An Essay on the Nature of the Matter Perspired and Absorbed From the Skin." In *Surgical and Physiological Essays*, 107–165. Printed for James Evans.

Aiello, L. C. 1992. "Allometry and the Analysis of Size and Shape in Human Evolution." *Journal of Human Evolution* 22, no. 2: 127–147. https://doi.org/10.1016/0047-2484(92)90034-7.

Blackburn, T. M., and B. A. Hawkins. 2004. "Bergmann's Rule and the Mammal Fauna of Northern North America." *Ecography* 27, no. 6: 715–724. https://doi.org/10.1111/j.0906-7590.2004.03999.x.

Bogin, B., M. Hermanussen, and C. Scheffler. 2022. "Bergmann's Rule Is a "Just-So" Story of Human Body Size." *Journal of Physiological Anthropology* 41, no. 1: 1–13. https://doi.org/10.1186/s40101-022-00287-z.

Boyd, E. 1935. *The Growth of the Surface Area of the Human Body*. University of Minnesota Press.

Bretschneider, T., U. Koop, V. Schreiner, H. Wenck, and S. Jaspers. 2009. "Validation of the Body Scanner as a Measuring Tool for a Rapid Quantification of Body Shape." *Skin Research and Technology* 15, no. 3: 364–369. https://doi.org/10.1111/j.1600-0846.2009.00374.x.

Brožek, J., J. Pařízková, J. Mendez, and H. L. Barkett. 1987. "The Evaluation of Body Surface, Body Volume and Body Composition in Human Biology Research." *L'Anthropologie* 25, no. 3: 235–259.

Churchill, S. E. 2006. "Bioenergetic Perspectives on Neanderthal Thermoregulatory and Activity Budgets." In *Vertebrate Paleobiology and Paleoanthropology*, 113–133. Springer.

Collard, M., and A. Cross. 2017. "Thermoregulation in *Homo erectus* and the Neanderthals: A Reassessment Using a Segmented Model." In *Human Paleontology and Prehistory*, edited by A. Marom and E. Hovers, 161–174. Springer International Publishing.

Crawford, J. D., M. E. Terry, and G. M. Rourke. 1950. "Simplification of Drug Dosage Calculation by Application of the Surface Area Principle." *Pediatrics* 5, no. 5: 783–790.

Cross, A., M. Collard, and A. Nelson. 2008. "Body Segment Differences in Surface Area, Skin Temperature and 3D Displacement and the Estimation of Heat Balance During Locomotion in Hominins." *PLoS One* 3, no. 6: e2464. https://doi.org/10.1371/journal.pone.0002464.

Custor, J. 1873. "Ueber die relative grösse des darmkanales und der hauptsächlichsten körpersysteme beim menschen und bei wirbelthieren." *Archiv Für Anatomie, Physiologie Und Wissenschaftliche Medicin* 40: 478–504.

Dechenaud, M. E., S. Kennedy, S. Sobhiyeh, J. Shepherd, and S. B. Heymsfield. 2021. "Total Body and Regional Surface Area: Quantification With Low-Cost Three-Dimensional Optical Imaging Systems." *American Journal of Physical Anthropology* 175, no. 4: 865–875. https://doi.org/10.1002/ajpa.24243.

DuBois, D., and E. F. DuBois. 1916. "A Formula to Estimate the Approximate Surface Area if Height and Weight Be Known." *Archives of Internal Medicine* 17: 863–871.

Felici, A., J. Verweij, and A. Sparreboom. 2002. "Dosing Strategies for Anticancer Drugs: The Good, the Bad and Body-Surface Area." *European Journal of Cancer* 38, no. 13: 1677–1684.

Fetter, V., M. Prokopec, J. Suchý, and S. Titlbachová. 1967. *Antropologie*. 1st ed. Academia.

Fubini, S., and J. Ronchi. 1881. "Ueber die perspiration der kohlensaure beim menschen." *Moleschtt's Untersuchungen zur Naturlehre des Menschen* 12: 1–30.

Gehan, E. A., and S. L. George. 1970. "Estimation of Human Body Surface Area From Height and Weight." *Cancer Chemotherapy Reports* 57: 225–235.

Geist, V. 1990. "Bergmann's Rule Is Invalid: A Reply to J. D. Paterson." *Canadian Journal of Zoology* 68, no. 7: 1613–1615. https://doi.org/10.1139/z90-241.

Haycock, G. B., G. J. Schwartz, and D. H. Wisotsky. 1978. "Geometric Method for Measuring Body Surface Area: A Height-Weight Formula Validated in Infants, Children, and Adults." *Journal of Pediatrics* 93, no. 1: 62–66. https://doi.org/10.1016/S0022-3476(78)80601-5.

Hora, M., H. Pontzer, M. Struška, P. Entin, and V. Sládek. 2022. "Comparing Walking and Running in Persistence Hunting." *Journal of Human Evolution* 172: 103247. https://doi.org/10.1016/j.jhevol.2022.103247.

Hora, M., H. Pontzer, C. M. Wall-Scheffler, and V. Sládek. 2020. "Dehydration and Persistence Hunting in *Homo erectus*." *Journal of Human Evolution* 138: 102682. https://doi.org/10.1016/j.jhevol.2019.102682.

Hosey-Cojocari, C., S. S. Chan, C. S. Friesen, et al. 2021. "Are Body Surface Area Based Estimates of Liver Volume Applicable to Children With Overweight or Obesity? An in Vivo Validation Study." *Clinical and Translational Science* 14, no. 5: 2008–2016. https://doi.org/10.1111/cts.13059.

Hsu, Y.-W., and C.-Y. Yu. 2010. "Hand Surface Area Estimation Formula Using 3D Anthropometry." *Journal of Occupational and Environmental Hygiene* 7, no. 11: 633–639. https://doi.org/10.1080/15459624.2010.514259.

Kasabova, B. E., and T. W. Holliday. 2015. "New Model for Estimating the Relationship Between Surface Area and Volume in the Human Body Using Skeletal Remains: Modeling Surface Area and Volume in Humans." *American Journal of Physical Anthropology* 156, no. 4: 614–624. https://doi.org/10.1002/ajpa.22678.

Katzmarzyk, P. T., and W. R. Leonard. 1998. "Climatic Influences on Human Body Size and Proportions: Ecological Adaptations and Secular Trends." *American Journal of Physical Anthropology* 106, no. 4: 483–503. https://doi.org/10.1002/(SICI)1096-8644(199808)106:4<483::AID-AJPA4>3.0.CO;2-K.

Knussmann, R. 1988. "Somatometrie." In *Anthropologie: Handbuch der vergleichenden biologie des menschen*, edited by R. Knussmann, 232–285. Gustav Fischer Verlag.

Kordsmeyer, T. L., J. Hunt, D. A. Puts, J. Ostner, and L. Penke. 2018. "The Relative Importance of Intra-and Intersexual Selection on Human

Male Sexually Dimorphic Traits." *Evolution and Human Behavior* 39: 424–436. https://doi.org/10.1016/j.evolhumbehav.2018.03.008.

Kordsmeyer, T. L., and L. Penke. 2019. "Effects of Male Testosterone and Its Interaction With Cortisol on Self-and Observer-Rated Personality States in a Competitive Mating Context." *Journal of Research in Personality* 78: 76–92. https://doi.org/10.1016/j.jrp.2018.11.001.

Kordsmeyer, T. L., J. Stern, and L. Penke. 2019. "3D Anthropometric Assessment and Perception of Male Body Morphology in Relation to Physical Strength." *American Journal of Human Biology* 31, no. 5: e23276. https://doi.org/10.1002/ajhb.23276.

Krzywicki, H. J., and K. S. K. Chinn. 1967. "Human Body Density and Fat of an Adult Male Population as Measured by Water Displacement." *American Journal of Clinical Nutrition* 20, no. 4: 305–310. https://doi.org/10.1093/ajcn/20.4.305.

Lee, J.-Y., J.-W. Choi, and H. Kim. 2007. "Determination of Hand Surface Area by Sex and Body Shape Using Alginate." *Journal of Physiological Anthropology* 26, no. 4: 475–483. https://doi.org/10.2114/jpa2.26.475.

Maijanen, H. 2009. "Testing Anatomical Methods for Stature Estimation on Individuals From the W. M. Bass Donated Skeletal Collection." *Journal of Forensic Sciences* 54, no. 4: 746–752. https://doi.org/10.1111/j.1556-4029.2009.01053.x.

Mathijssen, R. H. J., F. A. De Jong, W. J. Loos, J. M. Van Der Bol, J. Verweij, and A. Sparreboom. 2007. "Flat-Fixed Dosing Versus Body Surface Area–Based Dosing of Anticancer Drugs in Adults: Does It Make a Difference?" *Oncologist* 12, no. 8: 913–923. https://doi.org/10.1634/theoncologist.12-8-913.

Moore, R. A., P. Popowicz, and B. Burns. 2024. "Rule of Nines." In *StatPearls [Internet]*. Treasure Island.

Mosteller, R. D. 1987. "Simplified Calculation of Body-Surface Area." *New England Journal of Medicine* 317, no. 17: 1098–1098. https://doi.org/10.1056/NEJM198710223171717.

Ocobock, C. 2024. "Human Cold Adaptation: An Unfinished Agenda v2.0." *American Journal of Human Biology* 36, no. 3: e23937. https://doi.org/10.1002/ajhb.23937.

Pai, M. P. 2012. "Drug Dosing Based on Weight and Body Surface Area: Mathematical Assumptions and Limitations in Obese Adults." *Pharmacotherapy: The Journal of Human Pharmacology and Drug Therapy* 32, no. 9: 856–868. https://doi.org/10.1002/j.1875-9114.2012.01108.x.

Peters, A. M., and D. M. Glass. 2010. "Use of Body Surface Area for Assessing Extracellular Fluid Volume and Glomerular Filtration Rate in Obesity." *American Journal of Nephrology* 31, no. 3: 209–213. https://doi.org/10.1159/000271272.

Pierson, W. R. 1962. "The Estimation of Body Surface Area by Monophotogrammetry." *American Journal of Physical Anthropology* 20, no. 3: 399–402. https://doi.org/10.1002/ajpa.1330200326.

Pineau, J.-C., and F. V. Ramirez Rozzi. 2022. "Measuring Body Fat—How Accurate Is the Extrapolation of Predictive Models in Epidemiology?" *PLoS One* 17, no. 2: e0263590. https://doi.org/10.1371/journal.pone.0263590.

Pinkel, D. 1958. "The Use of Body Surface Area as a Criterion of Drug Dosage in Cancer Chemotherapy." *Cancer Research* 18: 853–856.

Pomeroy, E., J. T. Stock, and J. C. K. Wells. 2021. "Population History and Ecology, in Addition to Climate, Influence Human Stature and Body Proportions." *Scientific Reports* 11: 274. https://doi.org/10.1038/s41598-020-79501-w.

Raxter, M. H., B. M. Auerbach, and C. B. Ruff. 2006. "Revision of the Fully Technique for Estimating Statures." *American Journal of Physical Anthropology* 130, no. 3: 374–384. https://doi.org/10.1002/ajpa.20361.

Retrouvey, H., J. Chan, and S. Shahrokhi. 2018. "Comparison of Two-Dimensional Methods Versus Three-Dimensional Scanning Systems in the Assessment of Total Body Surface Area Estimation in Burn Patients." *Burns* 44, no. 1: 195–200. https://doi.org/10.1016/j.burns.2017.07.003.

Robertson, J. 1757. "An Essay Towards Ascertaining the Specific Gravity of Living Men." *Philosophical Transactions of the Royal Society of London* 50: 30–35.

Roussy, B. 1899. "Nouvelle méthode de mensuration directe de la surface de la peau humaine, etc., au moyen d'un nouvel appareil: Le pelliplanimétre a compteur totalisateur et á surface variable." *Comptes Rendus des Seances de la Societe de Biologie et de Ses Filiales* 51: 375–377.

Ruff, C. B. 1991. "Climate and Body Shape in Hominid Evolution." *Journal of Human Evolution* 21, no. 2: 81–105. https://doi.org/10.1016/0047-2484(91)90001-C.

Ruff, C. B. 1993. "Climatic Adaptation and Hominid Evolution: The Thermoregulatory Imperative." *Evolutionary Anthropology* 2, no. 2: 53–60. https://doi.org/10.1002/evan.1360020207.

Ruff, C. B. 1994. "Morphological Adaptation to Climate in Modern and Fossil Hominids." *American Journal of Physical Anthropology* 37, no. S19: 65–107. https://doi.org/10.1002/ajpa.1330370605.

Ruff, C. B., B. M. Holt, M. Niskanen, et al. 2012. "Stature and Body Mass Estimation From Skeletal Remains in the European Holocene." *American Journal of Physical Anthropology* 148, no. 4: 601–617. https://doi.org/10.1002/ajpa.22087.

Ruff, C. B., and B. A. Wood. 2023. "The Estimation and Evolution of Hominin Body Mass." *Evolutionary Anthropology: Issues, News, and Reviews* 32, no. 4: 223–237. https://doi.org/10.1002/evan.21988.

Ruxton, G. D., and D. M. Wilkinson. 2011. "Thermoregulation and Endurance Running in Extinct Hominins: Wheeler's Models Revisited." *Journal of Human Evolution* 61, no. 2: 169–175. https://doi.org/10.1016/j.jhevol.2011.02.012.

Sappey, P. C. 1852. *Traité d'anatomie descriptive*. Victor Masson.

Sendroy, J., and L. P. Cecchini. 1959. "Indirect Estimation of Body Surface Area and Volume." *Journal of Applied Physiology* 14, no. 6: 1000–1004. https://doi.org/10.1152/jappl.1959.14.6.1000.

Sendroy, J., and H. A. Collison. 1966. "Determination of Human Body Volume From Height and Weight." *Journal of Applied Physiology* 21, no. 1: 167–172.

Siri, W. E. 1961. "Body Volume Measurement by Gas Dilution." In *Techniques for Measuring Body Composition*, edited by J. Brožek and A. Henschel, 108–117. National Academy of Sciences, National Research Council.

Sládek, V., M. Berner, P. Galeta, L. Friedl, and Š. Kudrnová. 2010. "Technical Note: The Effect of Midshaft Location on the Error Ranges of Femoral and Tibial Cross-Sectional Parameters." *American Journal of Physical Anthropology* 141, no. 2: 325–332. https://doi.org/10.1002/ajpa.21153.

Sokal, R. R., and F. J. Rohlf. 1995. *Biometry: The Principles and Practice of Statistics in Biological Research*. 3rd ed. W. H. Freeman and Company.

Stibel, J. M. 2023. "Climate Change Predictive of Body Size and Proportionality in Humans." *Evolutionary Biology* 50, no. 4: 461–475. https://doi.org/10.1007/s11692-023-09616-1.

Tikuisis, P., P. Meunier, and C. E. Jubenville. 2001. "Human Body Surface Area: Measurement and Prediction Using Three Dimensional Body Scans." *European Journal of Applied Physiology* 85, no. 3–4: 264–271. https://doi.org/10.1007/s004210100484.

Vauthey, J. 2002. "Body Surface Area and Body Weight Predict Total Liver Volume in Western Adults." *Liver Transplantation* 8, no. 3: 233–240. https://doi.org/10.1053/jlts.2002.31654.

Wakat, D. K., R. E. Johnson, H. J. Krzywicki, and L. I. Gerber. 1971. "Correlation Between Body Volume and Body Mass in Men." *American*

Journal of Clinical Nutrition 24, no. 11: 1308–1312. https://doi.org/10.1093/ajcn/24.11.1308.

Wheeler, P. E. 1984. "The Evolution of Bipedality and Loss of Functional Body Hair in Hominids." *Journal of Human Evolution* 13, no. 1: 91–98. https://doi.org/10.1016/S0047-2484(84)80079-2.

Wheeler, P. E. 1992. "The Thermoregulatory Advantages of Large Body Size for Hominids Foraging in Savannah Environments." *Journal of Human Evolution* 23, no. 4: 351–362. https://doi.org/10.1016/0047-2484(92)90071-G.

Yu, C.-Y., Y.-W. Hsu, and C.-Y. Chen. 2008. "Determination of Hand Surface Area as a Percentage of Body Surface Area by 3D Anthropometry." *Burns* 34, no. 8: 1183–1189. https://doi.org/10.1016/j.burns.2008.03.010.

Yu, C.-Y., C.-H. Lin, and Y.-H. Yang. 2010. "Human Body Surface Area Database and Estimation Formula." *Burns* 36, no. 5: 616–629. https://doi.org/10.1016/j.burns.2009.05.013.

Supporting Information

Additional supporting information can be found online in the Supporting Information section. **Figure S1:** Bland–Altman analysis of body surface area (BSA) and body volume (BV) estimates generated by our models (top two rows) and by previously published models (bottom two rows). Differences between methods (*Y*-axis) are expressed as a percentage of the scanned value; accordingly, the bias values correspond to the mean percentage difference (%MD) reported in Tables 8 and 9. The solid line represents the ordinary least squares fit (in case of slope being significantly different from zero), with shaded areas indicating the 95% confidence interval. **Figure S2:** Relationship between stature and body mass in our sample 14 (both sample mean and individual data points are shown) and other male samples from five ecogeographic regions (only means are shown, solid line: reduced major axis regression; Ruff 1994). **Figure S3:** Bivariate distributions showing the relationships between the mean percentage difference (%MD) of body surface area (BSA) estimates and variables representing body size and proportions. Lower limb length is defined in Table 1, and trunk height and bi-iliac breadth are both defined in Table 4. Pearson correlation analysis revealed no statistically significant associations in any of the models. The analysis had 80% statistical power to detect an effect size of $r \geq 0.511$. **Figure S4:** Bivariate distributions showing the relationships between the mean percentage difference (%MD) of body volume (BV) estimates and variables representing body size and proportions (as described in Figure S3). Pearson correlation analysis revealed no statistically significant associations in any of the models. The analysis had 80% statistical power to detect an effect size of $r \geq 0.511$.